11-2006

Actinobacillus Actinomycetemcomitans Leukotoxin Requires Lipid Microdomains for Target Cell Cytotoxicity

Karen P. Fong

Cinthia M.F. Pacheco

Linda T. Otis

Samesh Baranwal

Irene R. Keiba

See next page for additional authors

Recommended Citation

Fong, K. P., Pacheco, C. M., Otis, L. T., Baranwal, S., Keiba, I. R., Harrison, G., Hersh, E. V., Boesze-Battaglia, K., & Lally, E. T. (2006). Actinobacillus Actinomycetemcomitans Leukotoxin Requires Lipid Microdomains for Target Cell Cytotoxicity. *Cell Microbiology, 8* (11), 1753-1767. http://dx.doi.org/10.1111/j.1462-5822.2006.00746.x

Actinobacillus Actinomycetemcomitans Leukotoxin Requires Lipid Microdomains for Target Cell Cytotoxicity

Abstract

Actinobacillus actinomycetemcomitans produces a leukotoxin (Ltx) that kills leukocyte function-associated antigen-1 (LFA-1)-bearing cells from man, the Great Apes and Old World monkeys. The unique specificity of Ltx for the β2 integrin, LFA-1, suggests it is capable of providing insight into the pathogenic mechanisms of Ltx and other RTX toxins. Using the Jurkat T cell line and an LFA-1-deficient Jurkat mutant (Jβ2.7) as models, we found the initial effect of Ltx is to elevate cytosolic Ca^{2+} $[Ca^{2+}]_c$, an event that is independent of the Ltx/LFA-1 interaction. $[Ca^{2+}]_c$ increases initiate a series of events that involve the activation of calpain, talin cleavage, mobilization to, and subsequent clustering of, LFA-1 in cholesterol and sphingolipid-rich regions of the plasma membrane known as lipid rafts. The association of Ltx and LFA-1 within lipid rafts is essential for cell lysis. Jβ2.7 cells fail to accumulate Ltx in their raft fractions and are not killed, while cholesterol depletion experiments demonstrate the necessity of raft integrity for Ltx function. We propose that toxin-induced Ca^{2+} fluxes mobilize LFA-1 to lipid rafts where it associates with Ltx. These findings suggest that Ltx utilizes the raft to stimulate an integrin signalling pathway that leads to apoptosis of target cells.

Disciplines

Dentistry

Author(s)

Karen P. Fong, Cinthia M.F. Pacheco, Linda T. Otis, Samesh Baranwal, Irene R. Keiba, Gerald Harrison, Elliot V. Hersh, Kathleen Boesze-Battaglia, and Edward T. Lally

Published in final edited form as:
Cell Microbiol. 2006 November ; 8(11): 1753–1767. doi:10.1111/j.1462-5822.2006.00746.x.

Actinobacillus actinomycetemcomitans leukotoxin requires lipid microdomains for target cell cytotoxicity

Karen P. Fong, **Cinthia M. F. Pacheco**, **Linda L. Otis**, **Somesh Baranwal**, **Irene R. Kieba**, **Gerald Harrison**, **Elliot V. Hersh**, **Kathleen Boesze-Battaglia**, and **Edward T. Lally***
The Leon Levy Research Center for Oral Biology, University of Pennsylvania, Philadelphia, PA 19104-6002, USA.

Summary

Actinobacillus actinomycetemcomitans produces a leukotoxin (Ltx) that kills leukocyte function-associated antigen-1 (LFA-1)-bearing cells from man, the Great Apes and Old World monkeys. The unique specificity of Ltx for the β2 integrin, LFA-1, suggests it is capable of providing insight into the pathogenic mechanisms of Ltx and other RTX toxins. Using the Jurkat T cell line and an LFA-1-deficient Jurkat mutant (Jβ2.7) as models, we found the initial effect of Ltx is to elevate cytosolic Ca^{2+} $[Ca^{2+}]_c$, an event that is independent of the Ltx/LFA-1 interaction. $[Ca^{2+}]_c$ increases initiate a series of events that involve the activation of calpain, talin cleavage, mobilization to, and subsequent clustering of, LFA-1 in cholesterol and sphingolipid-rich regions of the plasma membrane known as lipid rafts. The association of Ltx and LFA-1 within lipid rafts is essential for cell lysis. Jβ2.7 cells fail to accumulate Ltx in their raft fractions and are not killed, while cholesterol depletion experiments demonstrate the necessity of raft integrity for Ltx function. We propose that toxin-induced Ca^{2+} fluxes mobilize LFA-1 to lipid rafts where it associates with Ltx. These findings suggest that Ltx utilizes the raft to stimulate an integrin signalling pathway that leads to apoptosis of target cells.

Introduction

Actinobacillus actinomycetemcomitans produces a 116 kDa leukotoxin (Ltx) that is a member of the RTX (Repeats in ToXin) family (Welch, 1991) of cytolytic proteins and has a unique specificity for human immune cells (Taichman *et al*., 1987). A paradigm observed with many bacterial protein toxins is that target cell recognition (Parker *et al*., 1990; Van Rie *et al*., 1990; London, 1992; Merritt and Hol, 1995) initiates a multistep process that results in cell death. Consistent with this model, several RTX cytolysins kill cells by attaching to leukocyte function-associated antigen-1 (LFA-1), a heterodimeric adhesion receptor formed by the non-covalent association of α (αL; CD11a) and β (β_2; CD18) subunits (Lally *et al*., 1997; Wang *et al*., 1998; Ambagala *et al*., 1999; Li *et al*., 1999). LFA-1 is uniquely expressed on the cell surfaces of innate and adaptive immune cells which explains, in part, the restricted cytotoxicity exhibited by the toxin for cells from man, the Great Apes, and Old World monkeys (Taichman *et al*., 1987).

Attachment of microorganisms to integrin heterodimers and entry into the cell through an endocytic vacuole is a virulence strategy used by various intracellular bacteria (Relman *et al*., 1990) and viruses (Wickham *et al*., 1993) to achieve entry into host cells. Receptor-mediated endocytosis of microbial pathogens is observed with a number of the 24 αβ

*For correspondence. lally@toxin.dental.upenn.edu; Tel. (+1) 215 898 5913; Fax (+1) 215 573 2050..

integrin heterodimers but does not appear to be a function associated with LFA-1. LFA-1 plays multiple roles in the immune response such as mediating the migration of T cells across endothelial cells, emigration from blood vessels (Warnock *et al.*, 1998), crawling in tissue (Dustin *et al.*, 1997), and formation of the immunological synapse (Dustin *et al.*, 1998). A complex signalling system that is bidirectional and reciprocal (Dustin *et al.*, 2004) is necessary to accomplish the immunological multitasking required of this integrin. The 'outside-in' signal initiated by intercellular adhesion molecule-1 (ICAM-1) binding to LFA-1 leads to integrin clustering and increased avidity for ligand, while its complementary 'inside-out' signal originates in the cytoplasm and results in conformational changes in LFA-1 and an increased affinity for ICAM-1 (Dustin and Springer, 1989). Regions of the target cell membrane that contain a non-random and asymmetrical distribution of cholesterol and sphingolipids (lipid rafts) appear to play a role in the activation process in that, following stimulation, LFA-1 accumulates in the lipid raft compartment (Leitinger and Hogg, 2002).

Here we test the hypothesis that the interaction between Ltx and LFA-1 results in target cell responses that mimic 'outside-in' integrin activation signals. We demonstrate that Ltx induces an elevation of $[Ca^{2+}]_c$ and activation of calpain, an intracellular Ca^{2+}-dependent cysteine protease, which cleaves talin, a protein that anchors LFA-1 to the cytoskeleton, allowing clustering of LFA-1 on the cell surface and lateral movement of the LFA-1/Ltx complex to the raft compartment. We show that Ltx is able to mobilize $[Ca^{2+}]_c$ in a mutant cell line that does not express LFA-1 but is immune to the lethal effects of the toxin, indicating that the initial phase of Ltx intoxication does not require an interaction of the toxin with LFA-1, but that LFA-1 is required for movement of the toxin to the lipid micro-domain. We demonstrate that intact lipid rafts are essential to Ltx cytotoxicity because dispersion of rafts with methyl-β-cyclodextrin (MβCD) abolishes the ability of Ltx to kill target cells and cytotoxicity is restored when the raft is reconstituted. Our findings directly demonstrate that the interaction of an RTX toxin with LFA-1 is not a simple toxin docking but contains many features of 'outside-in' integrin activation.

Results

Actinobacillus actinomycetemcomitans Ltx induces LFA-1 clustering in Jurkat (Jn.9) cells

To determine if the membrane distribution of LFA-1 is altered in Ltx-treated cells, toxin-treated cells were compared with untreated cells and cells treated with heat-inactivated leukotoxin (ΔLtx, 70°C, 60 min). Following staining with anti-CD11a mAb, the cells were examined by confocal microscopy (Fig. 1, Confocal Microscopy), and the fluorescence intensity of the membrane analysed using a standardized method (Stewart *et al.*, 1998). It was determined that a threshold intensity of 175 < 255 represented a significant value while intensity between 80 < 174 represented non-significant background staining. Images with the highest LFA-1 fluorescence intensity (i.e. in the pixel intensity range 175 < 255) are represented by red colour and white was used to represent those areas whose intensity was not significant (80 < 174; Fig. 1, Fluorescence Intensity). Unstimulated cells and cells treated with ΔLtx exhibited very little high intensity LFA-1 fluorescence (*red*) when compared with Ltx-treated cells. Statistical analysis (Kruskal–Wallis One Way ANOVA on Ranks) of these measurements confirmed that the increase in LFA-1 fluorescence intensity observed in Ltx-treated cells was significantly higher than in untreated cells or cells treated with ΔLtx ($P < 0.05$) (Table 1). The increases in LFA-1 fluorescence in the Ltx-treated cells can be explained by upregulation of LFA-1 expression or by clustering of the integrin. To differentiate between these two possibilities, we utilized FACS® analysis to measure the total surface LFA-1 expression of 10 000 cells from each experimental group. The FACS® data (Fig. 1, FACS® Analysis) demonstrated equal expression of LFA-1 across all

experimental groups thereby indicating that Ltx was inducing clustering of LFA-1 on target cells and not increasing expression of LFA-1 in the Ltx-treated group.

Ltx induces α4β 1 integrin clustering in Jn.9 and Jβ2.7 cells

We believe that the LFA-1 clustering we observe in toxin-treated cells is either the result of a direct interaction of Ltx with LFA-1 or Ltx is exerting a broader, non-specific effect on target cells. If Ltx is inducing generalized cell activation, then we would expect to observe clustering of other integrins as well. We tested this hypothesis by examining the ability of 10^{-9} M Ltx to induce clustering of another integrin, α4β1, using wild-type Jn.9 and Jβ2.7 cells (Weber *et al.*, 1997). Jβ2.7 cells do not express either component of the αβ heterodimer (CD11a or CD18) on the cell surface. The LFA-1 fluorescence signal in Jn.9 cells served as a positive control (Fig. 2). A statistically significant increase in LFA-1 signal was observed in Jn.9 cells treated with Ltx (0.0235 ± 0.0024; $P < 0.001$) over a corresponding untreated control (0.0079 ± 0.0009). Examination of the α4β1 fluorescence in Ltx-treated Jn.9 cells (0.0207 ± 0.0008), using the same experimental conditions, showed that the clustered distribution pattern of this integrin was similar to that observed for LFA-1 in Ltx-treated Jn.9 cells (0.0235 ± 0.0024). The ability of Ltx to cluster α4β1 (0.0209 ± 0.0016) in LFA-1-deficient, as well as LFA-1-expressing cells, is an indication that the integrin mobilization is not the result of a toxin/LFA-1 interaction. It is possible that the $[Ca^{2+}]_c$ increases that had been observed in intoxicated cells (Taichman *et al.*, 1991) might be responsible for these observations.

Ltx mobilizes $[Ca^{2+}]_c$ in the absence of LFA-1

We explored the effect of $[Ca^{2+}]_c$ increases in LFA-1 clustering utilizing wild-type Jn.9 cells and two Jn.9 mutants (Weber *et al.*, 1997): Jβ2.7, an LFA-1-deficient cell line, and Jβ2.7/hCD11a, a cell line produced by transfecting Jβ2.7 cells with a human CD11a transgene resulting in the expression of wild-type levels of LFA-1 on their cell surfaces (Fig. 3A). The earliest observable effect of Ltx on all three cell lines was an elevation of $[Ca^{2+}]_c$ (Fig. 3B) which occurred within 60 s after addition of the toxin to cultures. $[Ca^{2+}]_c$ increases were not observed when each corresponding cell line was exposed to ΔLtx. The Ltx-mediated elevation of $[Ca^{2+}]_c$ levels was decreased upon preincubation of the cells with 100 μM 2-aminoethoxy-diphenyl borate (2-APB), an efficient blocker of store operated Ca^{2+} entry, while no increases were observed in cells treated with 100 μM 2-APB and ΔLtx (Fig. 3C). The ability of the toxin to mobilize $[Ca^{2+}]_c$ in both LFA-1-positive and -negative cells indicates that this initial phase of Ltx intoxication does not require an interaction of the toxin with integrin.

We then examined the ability of Ltx to kill the three target cell lines (Fig. 3D) and found that while all cell lines had exhibited similar Ltx-induced $[Ca^{2+}]_c$ increases, only those cells expressing LFA-1 (Jn.9 and Jβ2.7/hCD11a) were killed in a dose-dependent manner as the Ltx concentration was increased from 10^{-9} M to 10^{-6} M. The results are consistent with a previous demonstration of passive adsorption of Ltx onto both toxin-sensitive cells and certain toxin-resistant cells (Simpson *et al.*, 1988) and indicates that while the interaction of Ltx with target cell membranes results in elevation of $[Ca^{2+}]_c$, the presence of the LFA-1 heterodimer appears to be critical for cell lysis.

Ltx-induced clustering of LFA-1 involves reorganization of the cytoskeleton

LFA-1 is dispersed throughout the non-raft compartment of the membrane as a result of its linkage to components of the cytoskeleton which both constrain lateral movement of the integrin and confine it to this partition. Therefore, the LFA-1 clustering we observed in the previous section could be the result of either a breakdown of the cytoskeletal attachment or, conversely, from the formation of new cytoskeletal connections. To determine which of

these possibilities is occurring in Ltx-treated cells, we investigated the effect of jasplakinolide, a compound that stabilizes pre-existing actin filaments and promotes actin polymerization (Bubb *et al.*, 2000), as well as the compound, cytochalasin D (cD), which disrupts the actin filament organization (Cooper, 1987).

We analysed the net LFA-1-fluorescence intensity from Jn.9 cells in each of our experimental and control groups to determine whether jasplakinolide affected the LFA-1 distribution of cells treated with Ltx (Fig. 4A and B). As expected, the net LFA-1 fluorescence intensity of cells stained with LFA-1 antibody (0.00595 ± 0.00181) increased over twofold following the addition of Ltx (0.0128 ± 0.00276) to cultures ($P < 0.01$). On the other hand, a 30 min preincubation with 1 μM jasplakinolide inhibited the Ltx induced clustering of LFA-1 (0.00620 ± 0.00136) to the level of cells pretreated with jasplakinolide alone (0.0058 ± 0.0004) or untreated control cells (0.00595 ± 0.00181). The results suggest that changes in the actin cytoskeleton occur in cells exposed to Ltx. The observation that the jasplakinolide and jasplakinolide plus Ltx experimental groups had LFA-1 fluorescence signals that were similar to untreated controls (Fig. 4B) is an indication that jasplakinolide is acting by blocking LFA-1 clustering and is not initiating receptor degradation. cD (4 μM) disrupts actin filament organization, freeing LFA-1 from cytoskeletal restraints resulting in an elevated LFA-1 signal in both cD (0.0126 ± 0.0014) and cD plus Ltx- (0.0119 ± 0.0011) treated cells that was similar to the level seen in cells exposed to Ltx (0.0128 ± 0.0012) (Fig. 4B).

The ability of jasplakinolide to prevent integrin clustering reinforces the notion that cytoskeletal reorganization is an early consequence of the interaction of toxin and target cell. LFA-1 mobilization is a critical component of integrin activation (Kucik *et al.*, 1996). Therefore, we examined the effect of pretreatment with either jasplakinolide or cD on Ltx cytotoxicity (Fig. 4C). Jasplakinolide-treated cells, exposed to Ltx, were not killed by the toxin as expected due to the ability of this compound to stabilize the cytoskeleton and prevent actin depolymerization. Contrary to our prediction, cD-treated cells were not killed by Ltx (Fig. 4C) despite integrin clustering indicating that integrin clustering by itself is not sufficient for Ltx cytotoxicity.

Talin, a protein that links LFA-1 to the cytoskeleton, is cleaved by calpain in Ltx-treated cells

Increases in $[Ca^{2+}]_c$ activate many cytoplasmic enzymes and mediators which have been implicated in integrin signalling and function. Previous studies have shown that the clustering of LFA-1 is initiated by Ca^{2+} mobilization which leads to activation of calpain, a cysteine protease (Stewart *et al.*, 1998). Activated calpain is capable of cleaving talin, a cytoskeletal protein that binds to the LFA-1 β chain cytoplasmic domain and tethers LFA-1 to the cytoskeleton (Kucik *et al.*, 1996). We examined the ability of Ltx-activated calpain to cleave talin, which would result in releasing LFA-1 from its cytoskeletal tether. Talin (250 kDa; Fig. 5A, untreated) was cleaved after a 30 min incubation with 10^{-9} M Ltx at 37°C, resulting in the appearance of a 47 kDa proteolytic fragment in lipid raft fractions isolated from Ltx-treated cells (Fig. 5A, Ltx). In contrast, no proteolytic cleavage product of talin was observed in the lipid raft fractions of Ltx-treated cells pretreated with 100 μM calpeptin (Fig. 5A, Calpeptin), a calpain inhibitor, for 30 min at 37°C. These findings suggest that addition of Ltx to target cells results in an increase in $[Ca^{2+}]_c$, which activates calpain and cleaves talin, freeing LFA-1 to move laterally within the plasma membrane.

As a follow-up experiment, we analysed the LFA-1 distribution in Ltx-treated cells pretreated with 100 μM calpeptin (Fig. 5B). When compared with Ltx-stimulated cells, untreated cells and cells pretreated with calpeptin showed significantly lower levels of high intensity fluorescence (Table 2, $P < 0.001$;). The results suggest that inhibition of the

cysteine protease, calpain, by calpeptin, results in LFA-1 bound to the cytoskeleton by talin, preventing its lateral movement within the membrane and decreased clustering. To determine if the addition of calpeptin had an effect on Ltx-mediated cytotoxicity (Fig. 5C), Jn.9 cells were subjected to 30 min pretreatments of 100, 33 10, 3.3 and 1 μM calpeptin before Ltx addition. Calpeptin treatment resulted in a in a dose-dependent inhibition of Ltx-mediated cytotoxicity.

Association of Ltx and LFA-1 with lipid microdomains

Sucrose density gradient centrifugation was used to deter mine the location of Ltx and LFA-1 in Ltx-treated and untreated cells. Significantly higher levels of LFA-1 and Ltx were detected in raft fractions in Jn.9 cells exposed to 10^{-9} M Ltx compared with untreated cells (Fig. 6A and B). By confocal microscopy, LFA-1 is shown to colocalize with the raft marker CD55 in Ltx-treated cells but not in untreated cells (Fig. 6C).

Although it has been possible to demonstrate the binding of Ltx to LFA-1 in pull down experiments (Lally *et al.*, 1997), the question arises as to whether the Ltx/LFA-1 interaction is the result of independent migration of each element to the raft compartment or if binding occurs outside the raft and the complex becomes raft associated. To address this question, we again used the LFA-1-deficient mutant Jβ2.7 and Jβ2.7/hCD11a in which LFA-1 expression had been restored by transfection. Lipid raft fractions of each cell line were examined for the presence of Ltx using polyclonal anti-Ltx antibody (Lally *et al.*, 1989a). Significantly lower amounts ($P < 0.05$) of Ltx were detected in lipid raft fractions of Jβ2.7 lacking LFA-1 compared with Jβ2.7/hCD11a cells, indicating that the presence of cell surface LFA-1 is required for Ltx to enter the raft compartment (Fig. 7).

Ltx does not disrupt the integrity of the lipid raft compartment of target cells

Having demonstrated the association of Ltx and LFA-1 with lipid rafts, we wanted to determine if toxin damages the raft. Jurkat cells were treated with Ltx for 1 h at 37°C, lysed by homogenization in Triton X-100 and separated by sucrose density gradient centrifugation. In both toxin-treated and -untreated cells, CD55, a glycosylphosphatidylinositol (GPI)-linked protein, was detected in raft fractions 2–7 (Fig. 8A), while the human transferrin receptor, CD71, was detected in non-raft fractions 8–10 (Fig. 8B). Using confocal microscopy, the raft marker CD55 colocalized with Ctx which binds specifically to the raft enriched glycosphingolipid, GM1 ganglioside (Fig. 8C). In contrast, the CD71 did not colocalize with cholera toxin. The ability to separate raft (CD55) and non-raft (CD71) proteins in the presence or absence of Ltx suggests that the toxin does not destroy the integrity of lipid rafts in Ltx-treated cells.

Cholesterol depletion blocks Ltx-mediated cytotoxicity

To determine if lipid raft integrity is necessary for Ltx to kill cells, we examined the effect of MβCD, an agent known to disrupt lipid rafts by removing cholesterol from the Jurkat cell membrane (Kilsdonk *et al.*, 1995). Jn.9 cells were subjected to three different MβCD treatments and their rafts were visualized by confocal microscopy (Fig. 9A). Untreated cells showed the typical patched appearance of rafts on the cell surface. In contrast, 10 mM MβCD treatment disrupted the integrity of the lipid rafts, resulting in greatly diminished GM1 ganglioside fluorescence. The specificity of cholesterol depletion on Ltx cytotoxicity is observed in cells treated with 5 mM MβCD plus 5 mM MβCD-cholesterol conjugates. Exposing the cells to the same concentration of MβCD as when cholesterol was depleted, while providing cholesterol in the form of MβCD-cholesterol conjugates, facilitates the incorporation of exogenous cholesterol into membranes resulting in restoration of membrane rafts to a level similar to untreated cells. In a final group, Jurkat T cells were treated first with 10 mM MβCD, washed and subjected to a second incubation with MβCD-cholesterol

conjugate (at 0.5 mM cholesterol). This treatment restored Ctx fluorescence to wild-type levels demonstrating that MβCD treatment does not damage cells and cholesterol depletion is reversible. Analysis of cellular cholesterol of the four cell groups showed that treatment of cells with 10 mM MβCD decreased cholesterol content approximately 50% from 1.86 ± 0.1 μM cholesterol/10^6 cells to 0.95 ± 0.08 μM cholesterol/10^6 cells when compared with untreated Jn.9 cells (Table 3) while treatment of cells with 5 mM MβCD decreased cholesterol content by approximately 30% compared with untreated cells. Cells treated with 5 mM MβCD plus 5 mM MβCD-cholesterol complex or cells treated with 10 mM MβCD to deplete cholesterol followed by repletion with MβCD-cholesterol complexes had levels which exceeded those of untreated cells.

Ltx treatment of these cell groups followed by a trypan blue exclusion assay (Fig. 9B) showed a marked decrease in the percentage cytotoxicity in Ltx-stimulated cells pretreated with 10 mM MβCD (12.4 ± 2.5%) compared with untreated cells (45.9 ± 2.1%) ($P < 0.01$) which was reversed with 5 mM MβCD plus 5 mM MβCD-cholesterol mix (52.8 ± 8.3%) and repletion of cholesterol with MβCD-cholesterol inclusion complexes at 0.5 mM cholesterol (53.1 ± 3.75%). The results suggest that cholesterol depletion by MβCD disrupts the cellular processes that are involved in Ltx-mediated cytotoxicity.

Discussion

Expression of LFA-1 on the target cell surface is necessary for several RTX cytolysins to kill cells (Lally *et al.*, 1997; Wang *et al.*, 1998; Ambagala *et al.*, 1999; Li *et al.*, 1999). In the current study, we used Ltx as a model to identify and characterize the early steps in RTX intoxication in a Jurkat T cell line. The addition of Ltx to cells results in an aggregation of LFA-1 on the target cell surface (Fig. 1). The ability of Ltx to elevate $[Ca^{2+}]_c$ levels (Taichman *et al.*, 1991) and heat inactivation to ablate these changes suggests that the clustering of both LFA-1 and another integrin, α4β1 (Fig. 2), are part of the initial effect that the toxin has on the cell. Furthermore, Ltx induced increases in $[Ca^{2+}]_c$ (Fig. 3B) as well as clustering of α4β1 in Jβ2.7, an LFA-1-deficient Jurkat mutant, indicates that the integrin mobilization observed in our studies is the result of increased $[Ca^{2+}]_c$ levels and is not dependent upon an interaction of Ltx and LFA-1.

Elevations of $[Ca^{2+}]_c$ are not uncommon responses to bacterial protein toxins and have been reported in cells exposed to both multivalent and pore-forming toxins (Fivaz *et al.*, 1999; Tran Van Nhieu *et al.*, 2004). For example, *Aeromonas* aerolysin and *Listeria* listeriolysin, are secreted as monomers and assemble on the cell surface forming a transmembrane pore through which Ca^{2+} passes into the cytosol. However, the ability of Ltx to increase $[Ca^{2+}]_c$ levels in both toxin-sensitive and toxin-resistant cells (Fig. 3B) is provocative, suggesting that rather than forming a transmembrane pore, Ltx is initiating release of Ca^{2+} from internal stores. The ability of 2-APB (Bootman *et al.*, 2002), a reliable blocker of store-operated Ca^{2+} pathways, to inhibit these increases (Fig. 3C) reinforces this premise and is consistent with observations made with other RTX toxins (Uhlen *et al.*, 2000; Cudd *et al.*, 2003). The fact that Ltx stimulates $[Ca^{2+}]_c$ elevations of equal magnitudes in both toxin-sensitive cells, such as wild-type Jn.9 and LFA-1-reconstituted Jβ2.7/hCD11a cells, and the toxin-resistant Jβ2.7 cells (Fig. 3B), suggests that a simple elevation of $[Ca^{2+}]_c$, is probably not responsible for cell death but is a prelude for additional downstream events that are required for cytolysis.

In inactive immune cells, LFA-1 molecules are dispersed throughout the membrane and their lateral mobility is restricted by attachment to the cytoskeleton. Integrin clustering therefore implies that cytoskeletal reorganization is occurring in Ltx-treated cells. Stabilization of existing actin filaments and stimulating *de novo* actin polymerization by

pretreatment of target cells with jasplakinolide inhibited both clustering and cell death (Fig. 4), indicating that mobilization of LFA-1 is necessary for cytolysis. On the other hand, cD, disassembles the actin cytoskeleton resulting in increased LFA-1 clustering in both untreated controls and Ltx-treated cells. However, in spite of the clustering, cD-treated cells were also impervious to the effects of the toxin suggesting that while both Ltx and cD treatment affect the cytoskeleton, changes induced by Ltx are different than the disassembly that occurs with cD. The reason for the resistance of cD-treated cells to Ltx is not immediately clear. cD acts by capping the barbed ends of F-actin filaments thereby, preventing their lengthening (Cooper, 1987). As concentrations of F actin have been identified within raft membrane patches of Jurkat T cells (Harder and Simons, 1999), cytotoxicity may be dependent upon both LFA-1 mobilization and the integrity of these cD-sensitive lipid raft/cytoskeleton connections.

Toxins that utilize lipid rafts as part of their virulence schemes have receptors that are raft components (Harder and Simons, 1999; Brown and London, 2000). Interactions of Ltx and lipid rafts differ from the paradigm of these toxins because integrins do not associate with lipid micro-domains until after cell activation (Stewart *et al.*, 1998; Leitinger and Hogg, 2002). Analysis of raft fractions from Ltx-treated LFA-1-expressing (Jn.9, Jβ2.7/hCD11a) and LFA-1-deficient mutant cells (Jβ2.7) show that only cells expressing LFA-1 accumulated Ltx in the raft, indicating that an interaction with LFA-1 is required for targeting Ltx to the raft (Fig. 7). At present, it is not known whether Ltx is binding to LFA-1 that is already clustered in the raft or if Ltx binds LFA-1 outside the raft and the complex becomes raft associated. The $[Ca^{2+}]_c$ increases described above appear to have a role in the movement of LFA-1 to the raft (Stewart *et al.*, 1998) through the activation of calpain. Through the use of calpeptin, a selective inhibitor of calpain, we identified talin, a 250 kDa homodimeric cytoskeletal protein, to be a substrate for activated calpain in Ltx-treated Jurkat cells. The major integrin-binding site lies within the talin head (Liu *et al.*, 2000) and calpain cleaves between the talin head (47 kDa) and rod (203 kDa) domain (Critchley, 2000). When compared with untreated or cells treated with calpeptin, the talin head domain was detected in rafts of Ltx-treated cells (Fig. 5A), indicating that activated calpain cleaves talin, physically releasing LFA-1 from cytoskeletal restraints and allowing movement of LFA-1 and the talin head domain to lipid rafts. Calpain inhibition by calpeptin also inhibited clustering and subsequent killing of toxin-treated cells (Fig. 5B and C). The fact that talin bound to integrin β tails is able to colocalize with activated integrins (Tadokoro *et al.*, 2003), suggests that cleavage of talin plays a critical role in the integrin activation by Ltx.

Toxin, integrin and lipid rafts sound an arpeggio that transition the Ltx reaction from an initial integrin activation stage, characterized by $[Ca^{2+}]_c$ increases and LFA-1 migration to rafts, to the lytic stage that results in the death of LFA-1-bearing cells. The mechanism by which this occurs remains to be elucidated. Aggregation of toxin and integrin in lipid rafts (Figs 6 and 7) could result in membrane damage and subsequent cell death, however, also possible, is that a signal through LFA-1 is upregulating the apoptotic machinery of the target cell. Integrins possess a classical cell signalling capability in the presence of their cognate ligand, however, some also produce a negative cell death promoting signal in its absence (Frisch and Screaton, 2001; Stupack, 2005). The role that β2 integrins play at the crossroads of immune function and cell death is only beginning to be understood.

Our studies provide an indication that Ltx-induced $[Ca^{2+}]_c$ increases are capable of influencing the mobilization of integrins. Calcium plays a pivotal role in immune cell functions through the activation of transcription factors that induce several key genes that modulate diverse genetic programs, including cell proliferation, cell differentiation, effector function and cell death (Teague *et al.*, 1999). Cellular Ca^{2+} signals generated during these interactions are the sequelae of complex interactions between a variety of Ca^{2+} reservoirs

that supply, and sinks that assimilate, this divalent cation. Our current analysis is but an initial snapshot into what appears to be a dynamic process initiated by Ltx and target cells. Additional studies designed at determining the source of the Ca^{2+} will provide valuable insight into what is a complex environment.

In summary, the interaction of Ltx with toxin-susceptible cells mimics integrin activation and results an enrichment of both toxin and LFA-1 in the lipid rafts of target cells. Subsequent cytoskeletal reorganization within the intact raft is essential for Ltx-mediated cytotoxicity.

Experimental procedures

Antibodies and reagents

Anti-Ltx was described previously (Lally *et al.*, 1989a,b). Anti-CD11a, clone G25.2; anti-CD55, clone IA10; and anti-CD71, clone M-A712, were purchased from BD Biosciences, Pharmingen (San Diego, CA); anti-α4β1, clone PS/2, from Chemicon International (Temecula, CA); Alexa Fluor®-647 conjugated Ctx subunit B, streptavidin, Alexa Fluor®-488 conjugated secondary antibodies from Invitrogen, Molecular Probes (Carlsbad, CA); anti-cholera toxin B-subunit, calpeptin, jasplakinolide, cD from Calbiochem (San Diego, CA); biotinylated anti-CD55 from R and D Systems (Minneapolis, MN); antitalin, clone TA205, from Upstate (Charlottesville, VA); MβCD, fatty acid free BSA, 2-APB and cholesterol from Sigma (St Louis, MI).

Cell lines

The LFA-1 expressing human T lymphoma Jurkat cell line, Jn.9, and the LFA-1-deletion mutant, Jβ2.7 (Weber *et al.*, 1997) were gifts from Dr Lloyd Klickstein, Harvard, MA. Jβ2.7/ hCD11a was created by cloning the human CD11a gene (a gift from Martyn Robinson, Celltech, Slough, UK) into the mammalian expression vector pCDNA6/ V5®(Invitrogen), and transfecting into Jβ2.7. All cells were maintained at 37°C under 5% CO_2 in RPMI 1640 (Mediatech Cellgro, Herndon, VA) containing 10% FCS, 0.1 mM MEM non-essential amino acids, 1× MEM vitamin solution, 2 mM L-glutamine and 50 μg ml^{-1} gentamicin. Transfected cells were screened and maintained in 5 μg ml^{-1} blasticidin.

Immunofluorescence labelling and raft patching

Cells (3×10^6) were incubated with 10 μg ml^{-1} anti-CD11a (clone G25.2) or anti-α4β1 (clone PS/2) antibody, with or without 10^{-9} M Ltx or heat-inactivated (70°C, 1 h) Ltx at 37°C for 30 min followed by detection with 5 μg ml^{-1} Alexa Fluor®-488 conjugated secondary antibodies. 1 μM jasplakinolide, 4 μM cD and 100 μM calpeptin were added to cells for 30 min at 37°C before Ltx treatment. Cells were mounted by centrifugation at 1015 *g* for 5 min onto Cell-Tak™-coated (BD Biosciences, San Diego, CA) 0.17 mm Delta T dishes (Fisher Scientific, Hampton, NH). Lipid raft aggregation or patching with 100 μg ml^{-1} Alexa Fluor®-647 conjugated cholera toxin subunit B and 0.5 mg ml^{-1} anti-cholera toxin subunit B IgG (1:150 dilution) in untreated or cholesterol depleted and repleted cells, and colocalization of lipid rafts with anti-CD55 and anti-CD71 were performed according to Leitinger and Hogg (Leitinger and Hogg, 2002).

Confocal microscopy and immunofluorescence quantification

Images were acquired with a Nikon Eclipse TE300 microscope (100× objective), connected to a Bio-Rad Radiance Confocal Scanning System and analysed using the Laser Sharp 2000 Software (Bio-Rad Laboratories, Hercules, CA). Optical images of cell sections (512 × 512 pixels) were digitally recorded. LFA-1 fluorescence in the pixel intensity range (175 < 255) (Meta-Morph® version 6.0, Molecular Devices, Sunnyvale, CA) was depicted in red while

fluorescence intensities in the pixel range (80 < 174) was depicted in white. Statistical analysis of LFA-1 fluorescence intensities was performed using SigmaStat® 3.1 (Systat® Software, Port Richmond, CA).

FACS®analysis

LFA-1 expression was determined by FACS® analysis utilizing TS1/22 or TS1/18 (ATCC, Rockville, MD) as described previously (Lally *et al.*, 1997).

Isolation and analysis of membrane rafts

Triton X-100-resistant membrane rafts were prepared from Ltx and calpeptin-treated cells as previously described (Seno *et al.*, 2001). Equal amounts of protein from each fraction were analysed by SDS-PAGE/Western and dot blotting, scanned with the Kodak Digital Science Image Station® using the program Kodak ID3.5, or with the Personal Densitometer SI using the Molecular Dynamics Software Version NT4 (Amersham Biosciences, Piscataway, NJ). The net fluorescence intensity from three separate experiments was plotted against fraction number. Lipid rafts of calpeptin-treated cells were precipitated in ice-cold MOPS buffer, centrifuged at 244 980 *g* for 45 min at 4°C and resuspended in MOPS buffer before subjecting to SDS-PAGE/Western blotting and detection with antitalin antibody.

Ltx-mediated cytotoxicity

The trypan blue cytotoxicity assay was described previously (Brogan *et al.*, 1994). To test for inhibition, the cells were pre-treated with 100, 33, 10, 3.3 and 1 μM calpeptin, 1 μM jasplakinolide or 4 μM cD for 30 min before addition of 10^{-9} M Ltx.

MβCD treatments

Cholesterol depletion and replenishment was performed as described (Leitinger and Hogg, 2002). Cholesterol concentration in lipid raft fractions of untreated and MβCD-treated cells was performed using the Amplex Red Cholesterol Assay Kit (Invitrogen), as described by the manufacturer's instructions.

Measurement of $[Ca^{2+}]_c$ levels

$[Ca^{2+}]_c$ levels were performed on indo-1-loaded target cells using a Hitachi F2500 Fluorescence Spectrophotometer with an excitation wavelength of 338 nm and emission wavelengths of 405 and 480 nm (Ali *et al.*, 2000).

Acknowledgments

We thank Dr Lloyd B. Klickstein of the Harvard Medical School for providing us with his Jn.9 and Jβ2.7 cell lines and Dr Martyn Robinson, Celltech, for the human CD11a cDNA. Sylvia Decker provided expert technical assistance with confocal microscopy and Bridget J. Gallagher analysed the digital images. Dr Joel Rosenbloom provided us with many helpful suggestions and criticisms during the preparation of the manuscript. Supported by DE09517 and DE12305.

References

Ali H, Ahamed J, Hernandez-Munain C, Baron JL, Krangel MS, Patel DD. Chemokine production by G protein-coupled receptor activation in a human mast cell line: roles of extracellular signal-regulated kinase and NFAT. J Immunol. 2000; 165:7215–7223. [PubMed: 11120854]

Ambagala TC, Ambagala AP, Srikumaran S. The leukotoxin of *Pasteurella haemolytica* binds to β2 integrins on bovine leukocytes. FEMS Microbiol Lett. 1999; 179:161–167. [PubMed: 10481101]

Bootman MD, Collins TJ, Mackenzie L, Roderick HL, Berridge MJ, Peppiatt CM. 2-aminoethoxydiphenyl borate (2-APB) is a reliable blocker of store-operated Ca^{2+} entry but an

inconsistent inhibitor of $InsP_3$-induced Ca^{2+} release. FASEB J. 2002; 16:1145–1150. [PubMed: 12153982]

Brogan JM, Lally ET, Poulsen K, Kilian M, Demuth DR. Regulation of *Actinobacillus actinomycetemcomitans* leukotoxin expression: analysis of the promoter regions of leukotoxic and minimally leukotoxic strains. Infect Immun. 1994; 62:501–508. [PubMed: 8300209]

Brown DA, London E. Structure and function of sphingolipid- and cholesterol-rich membrane rafts. J Biol Chem. 2000; 275:17221–17224. [PubMed: 10770957]

Bubb MR, Spector I, Beyer BB, Fosen KM. Effects of jasplakinolide on the kinetics of actin polymerization. An explanation for certain in vivo observations. J Biol Chem. 2000; 275:5163–5170. [PubMed: 10671562]

Cooper JA. Effects of cytochalasin and phalloidin on actin. J Cell Biol. 1987; 105:1473–1478. [PubMed: 3312229]

Critchley DR. Focal adhesions – the cytoskeletal connection. Curr Opin Cell Biol. 2000; 12:133–139. [PubMed: 10679361]

Cudd L, Clarke C, Clinkenbeard K. Contribution of intracellular calcium stores to an increase in cytosolic calcium concentration induced by *Mannheimia haemolytica* leukotoxin. FEMS Microbiol Lett. 2003; 225:23–27. [PubMed: 12900016]

Dustin ML, Springer TA. T-cell receptor cross-linking transiently stimulates adhesiveness through LFA-1. Nature. 1989; 341:619–624. [PubMed: 2477710]

Dustin ML, Bromley SK, Kan Z, Peterson DA, Unanue ER. Antigen receptor engagement delivers a stop signal to migrating T lymphocytes. Proc Natl Acad Sci USA. 1997; 94:3909–3913. [PubMed: 9108078]

Dustin ML, Olszowy MW, Holdorf AD, Li J, Bromley S, Desai N, et al. A novel adaptor protein orchestrates receptor patterning and cytoskeletal polarity in T-cell contacts. Cell. 1998; 94:667–677. [PubMed: 9741631]

Dustin ML, Bivona TG, Philips MR. Membranes as messengers in T cell adhesion signaling. Nat Immunol. 2004; 5:363–372. [PubMed: 15052266]

Fivaz M, Abrami L, van der Goot FG. Landing on lipid rafts. Trends Cell Biol. 1999; 9:212–213. [PubMed: 10354632]

Frisch SM, Screaton RA. Anoikis mechanisms. Curr Opin Cell Biol. 2001; 13:555–562. [PubMed: 11544023]

Harder T, Simons K. Clusters of glycolipid and glycosylphosphatidylinositol-anchored proteins in lymphoid cells: accumulation of actin regulated by local tyrosine phosphorylation. Eur J Immunol. 1999; 29:556–562. [PubMed: 10064071]

Kilsdonk EP, Yancey PG, Stoudt GW, Bangerter FW, Johnson WJ, Phillips MC, et al. Cellular cholesterol efflux mediated by cyclodextrins. J Biol Chem. 1995; 270:17250–17256. [PubMed: 7615524]

Kucik DF, Dustin ML, Miller JM, Brown EJ. Adhesion-activating phorbol ester increases the mobility of leukocyte integrin LFA-1 in cultured lymphocytes. J Clin Invest. 1996; 97:2139–2144. [PubMed: 8621804]

Lally ET, Golub EE, Kieba IR, Taichman NS, Rosenbloom J, Rosenbloom JC, et al. Analysis of the *Actinobacillus actinomycetemcomitans* leukotoxin gene. Delineation of unique features and comparison to homologous toxins. J Biol Chem. 1989a; 264:15451–15456. [PubMed: 2670940]

Lally ET, Kieba IR, Demuth DR, Rosenbloom J, Golub EE, Taichman NS, et al. Identification and expression of the *Actinobacillus actinomycetemcomitans* leukotoxin gene. Biochem Biophys Res Commun. 1989b; 159:256–262. [PubMed: 2647082]

Lally ET, Kieba I, Sato A, Green DR, Rosenbloom J, Korostoff J, et al. RTX toxins recognize a β2 inte-grin on the surface of human target cells. J Biol Chem. 1997; 272:30463–30469. [PubMed: 9374538]

Leitinger B, Hogg N. The involvement of lipid rafts in the regulation of integrin function. J Cell Sci. 2002; 115:963–972. [PubMed: 11870215]

Li J, Clinkenbeard KD, Ritchey JW. Bovine CD18 identified as a species specific receptor for *Pasteurella haemolytica* leukotoxin. Vet Microbiol. 1999; 67:91–97. [PubMed: 10414364]

Liu S, Calderwood DA, Ginsberg MH. Integrin cytoplasmic domain-binding proteins. J Cell Sci. 2000; 113(Pt 20):3563–3571. [PubMed: 11017872]

London E. Diphtheria toxin: membrane interaction and membrane translocation. Biochim Biophys Acta. 1992; 1113:25–51. [PubMed: 1550860]

Merritt EA, Hol WG. AB_5 toxins. Curr Opin Struct Biol. 1995; 5:165–171. [PubMed: 7648317]

Parker MW, Tucker AD, Tsernoglou D, Pattus F. Insights into membrane insertion based on studies of colicins. Trends Biochem Sci. 1990; 15:126–129. [PubMed: 2187292]

Relman D, Tuomanen E, Falkow S, Golenbock DT, Saukkonen K, Wright SD. Recognition of a bacterial adhesion by an integrin: macrophage CR3 (αMβ2, CD11b/CD18) binds filamentous hemagglutinin of *Bordetella pertussis*. Cell. 1990; 61:1375–1382. [PubMed: 2364431]

Seno K, Kishimoto M, Abe M, Higuchi Y, Mieda M, Owada Y, et al. Light- and guanosine 5′-3-O-(thio) triphosphate-sensitive localization of a G protein and its effector on detergent-resistant membrane rafts in rod photoreceptor outer segments. J Biol Chem. 2001; 276:20813–20816. [PubMed: 11319214]

Simpson DL, Berthold P, Taichman NS. Killing of human myelomonocytic leukemia and lymphocytic cell lines by *Actinobacillus actinomycetemcomitans* leukotoxin. Infect Immun. 1988; 56:1162–1166. [PubMed: 3258584]

Stewart MP, McDowall A, Hogg N. LFA-1-mediated adhesion is regulated by cytoskeletal restraint and by a Ca^{2+}-dependent protease, calpain. J Cell Biol. 1998; 140:699–707. [PubMed: 9456328]

Stupack DG. Integrins as a distinct subtype of dependence receptors. Cell Death Differ. 2005; 12:1021–1030. [PubMed: 15933741]

Tadokoro S, Shattil SJ, Eto K, Tai V, Liddington RC, de Pereda JM, et al. Talin binding to integrin β tails: a final common step in integrin activation. Science. 2003; 302:103–106. [PubMed: 14526080]

Taichman NS, Simpson DL, Sakurada S, Cranfield M, DiRienzo J, Slots J, et al. Comparative studies on the biology of *Actinobacillus actinomycetemcomitans* leukotoxin in primates. Oral Microbiol Immunol. 1987; 2:97–104. [PubMed: 3507626]

Taichman NS, Iwase M, Lally ET, Shattil SJ, Cunningham ME, Korchak HM, et al. Early changes in cytosolic calcium and membrane potential induced by *Actinobacillus actinomycetemcomitans* leukotoxin in susceptible and resistant target cells. J Immunol. 1991; 147:3587–3594. [PubMed: 1940358]

Teague TK, Hildeman D, Kedl RM, Mitchell T, Rees W, Schaefer BC, et al. Activation changes the spectrum but not the diversity of genes expressed by T cells. Proc Natl Acad Sci USA. 1999; 96:12691–12696. [PubMed: 10535984]

Tran Van Nhieu G, Clair C, Grompone G, Sansonetti P. Calcium signalling during cell interactions with bacterial pathogens. Biol Cell. 2004; 96:93–101. [PubMed: 15093131]

Uhlen P, Laestadius A, Jahnukainen T, Soderblom T, Backhed F, Celsi G, et al. α-Haemolysin of uropathogenic E. coli induces Ca^{2+} oscillations in renal epithelial cells. Nature. 2000; 405:694–697. [PubMed: 10864327]

Van Rie J, Jansens S, Hofte H, Degheele D, Van Mellaert H. Receptors on the brush border membrane of the insect midgut as determinants of the specificity of *Bacillus thuringiensis* δ-endotoxins. Appl Environ Microbiol. 1990; 56:1378–1385. [PubMed: 2339890]

Wang JF, Kieba IR, Korostoff J, Guo TL, Yamaguchi N, Rozmiarek H, et al. Molecular and biochemical mechanisms of *Pasteurella haemolytica* leukotoxin-induced cell death. Microb Pathog. 1998; 25:317–331. [PubMed: 9895270]

Warnock RA, Askari S, Butcher EC, von Andrian UH. Molecular mechanisms of lymphocyte homing to peripheral lymph nodes. J Exp Med. 1998; 187:205–216. [PubMed: 9432978]

Weber KS, York MR, Springer TA, Klickstein LB. Characterization of lymphocyte function-associated antigen 1 (LFA-1)-deficient T cell lines: the αL and β2 subunits are interdependent for cell surface expression. J Immunol. 1997; 158:273–279. [PubMed: 8977199]

Welch RA. Pore-forming cytolysins of gram-negative bacteria. Mol Microbiol. 1991; 5:521–528. [PubMed: 2046545]

Wickham TJ, Mathias P, Cheresh DA, Nemerow GR. Integrins $\alpha_v\beta_3$ and $a_v\beta_5$ promote adenovirus internalization but not virus attachment. Cell. 1993; 73:309–319. [PubMed: 8477447]

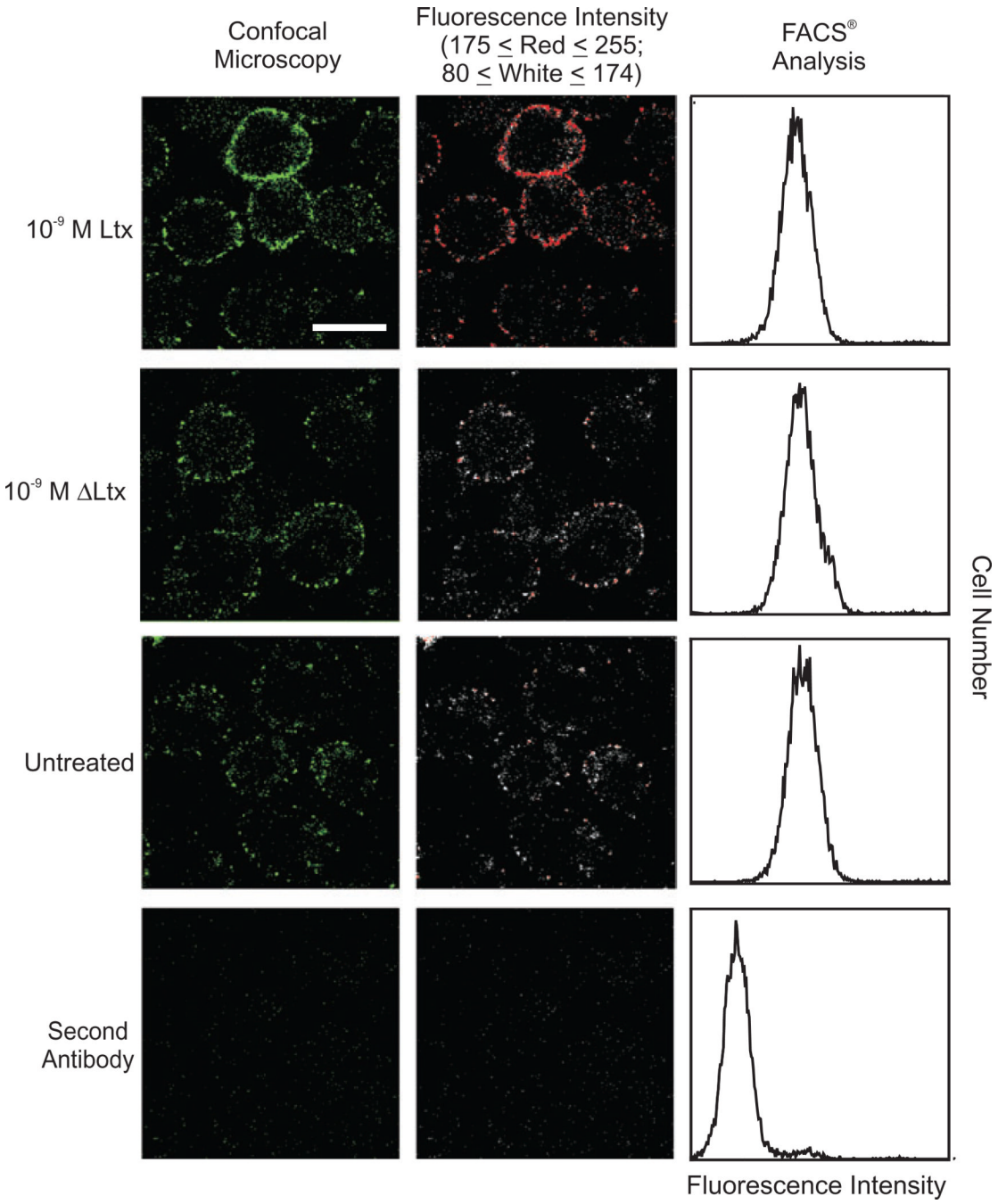

Fig. 1.

Clustering of LFA-1 in Ltx-treated cells. Jn.9 cells were incubated with 10^{-9} M Ltx or ΔLtx and 10 μg ml^{-1} anti-CD11a at 37°C for 30 min. The cells were fixed and stained with Alexa Fluor®-488 conjugated secondary antibody before visualizing by confocal microscopy under a 100× objective (left panel). When compared with untreated cells, cells treated with ΔLtx and cells stained only with secondary antibodies, Ltx-treated cells appeared to have focal increases in fluorescence intensity in the cell membrane. Fluorescence intensities for each sample were quantified using the Metamorph® 6.0 program and images in the pixel intensity range (< 174) are depicted in white while the pixel intensity range (175 < 255) are

in red (middle panel). An FACS® analysis was performed to measure total surface expression of LFA-1 of 10 000 cells from each group (right panel). Bar, 10 μm.

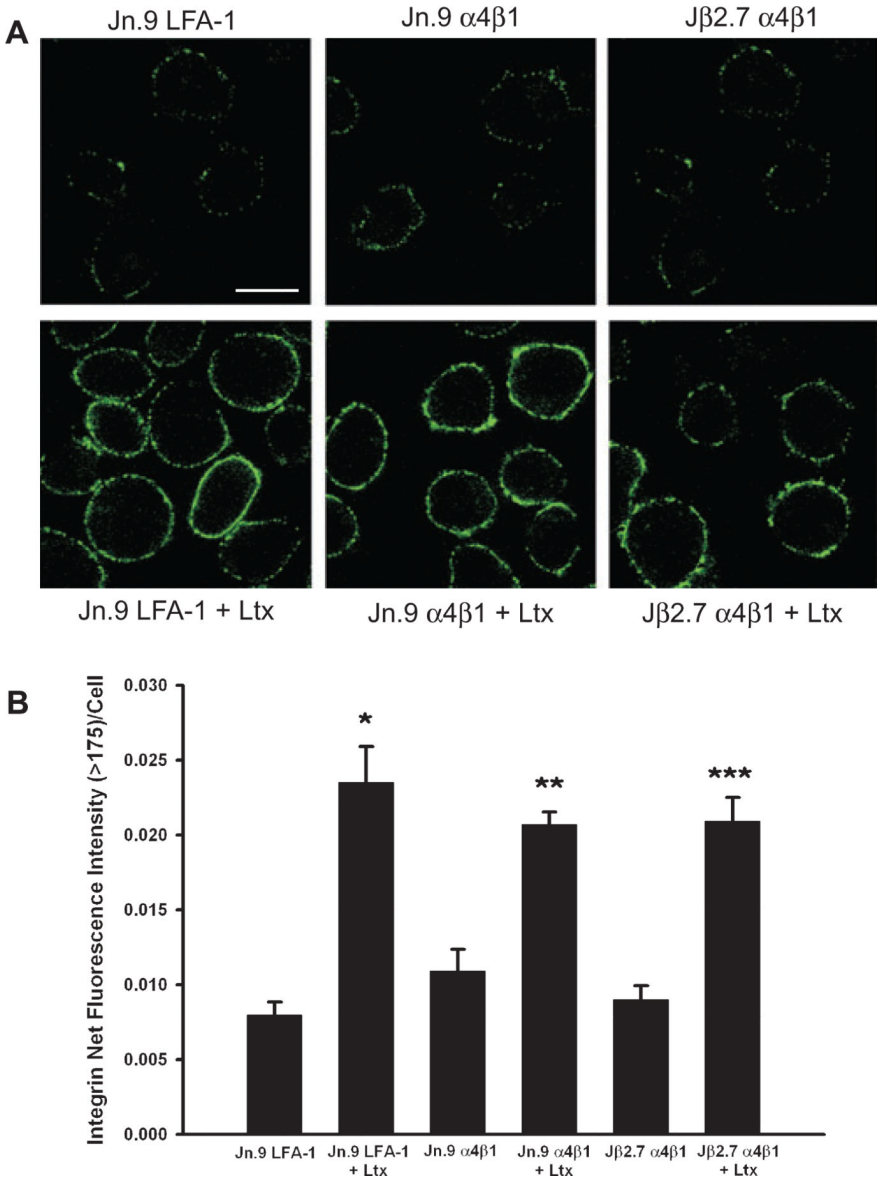

Fig. 2. Clustering of α4β1 integrin in Ltx-treated Jn.9 and Jβ2.7 cells

A. Cells were incubated as in Fig. 1 with 10 μg ml^{-1} anti-LFA-1 or anti-α4β1. When compared with untreated cells (top panel), LFA-1 and the α4β1 integrin appeared to be clustered on the cell membrane of both Jn.9 and Jβ2.7 Ltx-treated cells (bottom panel). Bar, 10 μm. B. The levels of fluorescence for each sample were quantified using the Metamorph® 6.0 Program. Statistical analysis was performed on 60 cells of each group. Values reported as mean ± SEM of at least seven determinations from a representative experiment. *$P < 0.001$ versus LFA-1-stained Jn.9 cells; **$P < 0.001$ versus α4β1-stained Jn.9 cells; ***$P < 0.001$ versus α4β1-stained Jβ2.7 cells.

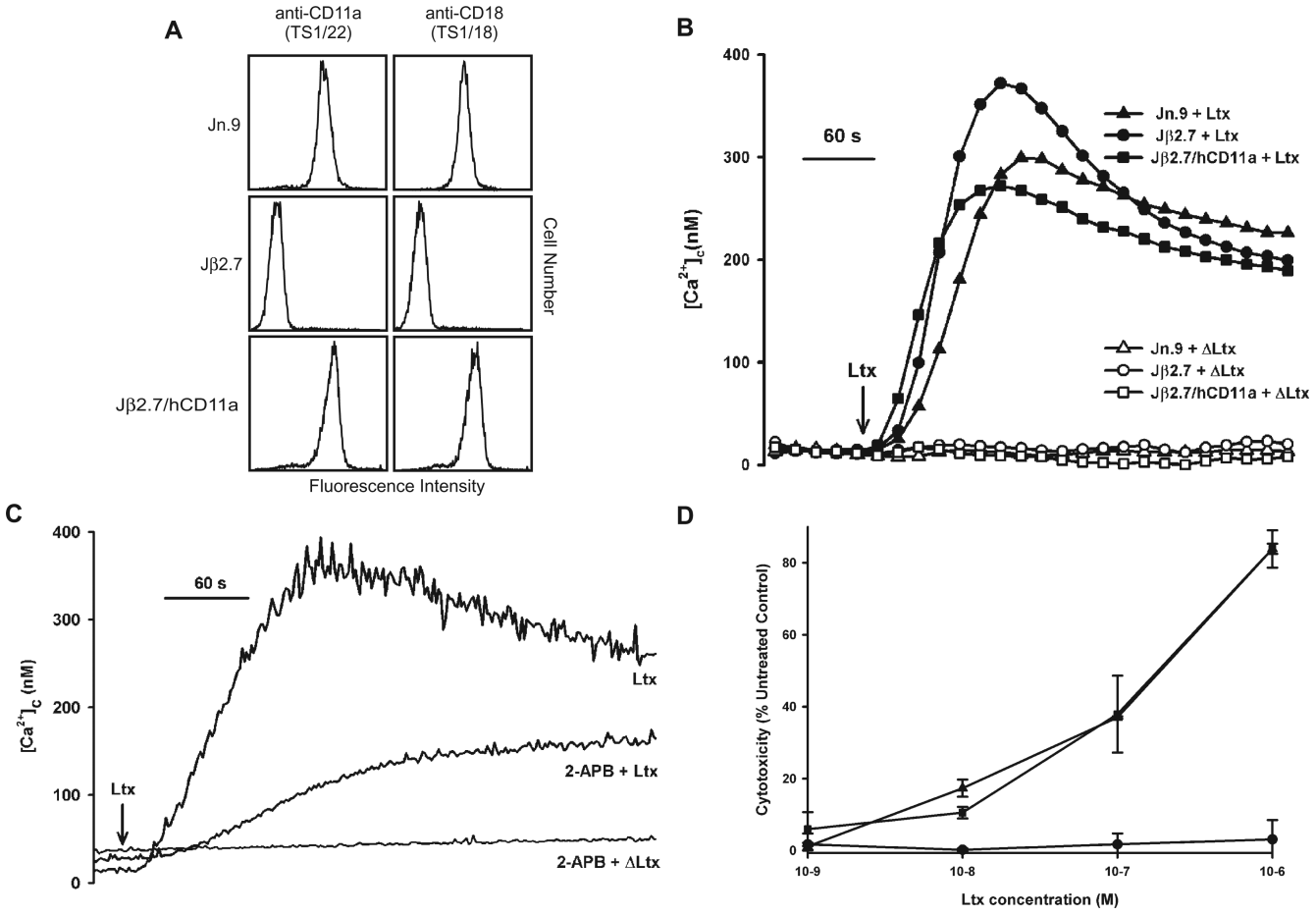

Fig. 3. Mobilization of $[Ca^{2+}]_c$ in Ltx-treated T cells

A. FACS® analysis of 10 000 cells in each group show that the CD11a transfected mutant Jβ2.7/hCD11a and the wild-type Jn.9 cells express both components of the LFA-1 heterodimer (CD11a and CD18) in contrast to the mutant, LFA-1-deficient Jβ2.7 cells.

B. An elevation of $[Ca^{2+}]_c$ was observed within 60 s after stimulation of Jn.9 (▲,△), Jβ2.7 (●○) and Jβ2.7/hCD11a (■, □) cells with 10^{-9} M Ltx (filled symbols) in contrast to cells treated with ΔLtx (open symbols).

C. Preincubation of Jn.9 cells with 100 μM 2-APB decreased Ltx-induced $[Ca^{2+}]_c$ increases while incubation with 2-APB with ΔLtx had no effect on $[Ca^{2+}]_c$ levels.

D. When Jn.9 (▲), Jβ2.7/hCD11a (■) and Jβ2.7 (●) cells were subjected to increasing (10^{-9} M to 10^{-6} M) concentrations of Ltx, cells expressing LFA-1 were killed in a dose-dependent manner compared with cells lacking LFA-1, suggesting that the initial elevation of $[Ca^{2+}]_c$ and Ltx-mediated cytotoxicity occur independently of each other.

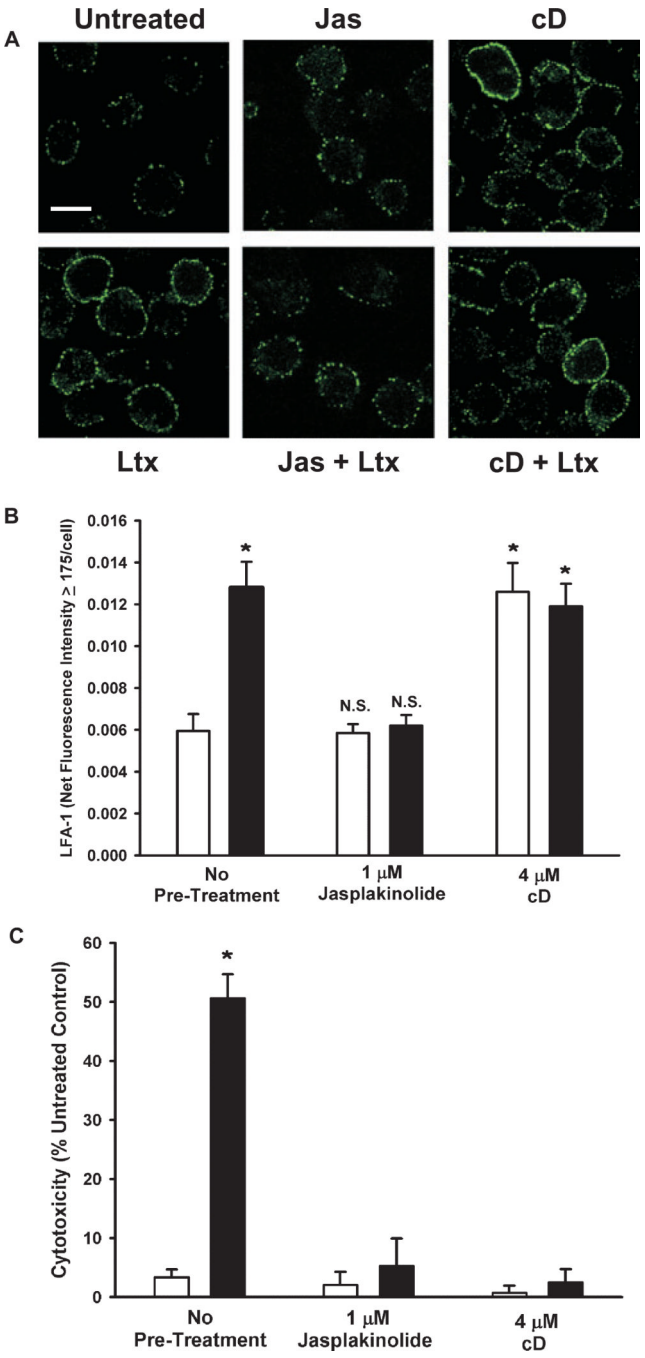

Fig. 4. Ltx induces reorganization of the actin cytoskeleton

A. Cells were treated with 1 μM jasplakinolide (Jas) or 4 μM cD prior to treatment with 10^{-9} M Ltx, and incubated with anti-CD11a mAb as described in Fig. 1. In the presence or absence of Ltx, jasplakinolide prevented LFA-1 clustering (middle panel). In contrast, cD promoted clustering of Ltx-treated and untreated cells (right panel). In the absence of jasplakinolide or cD, Ltx induced clustering of LFA-1 (left panel). Bar, 10 μm.

B. The level of LFA-1 fluorescence was determined as in Fig. 2. Ltx-treated cells (■); no Ltx (□). The LFA-1 fluorescence intensity in Ltx-treated cells is significantly higher than that of the untreated control and groups pretreated with jasplakinolide but showed similarly

high LFA-1 fluorescence intensities as compared with groups pretreated with cD. Values represent mean ± SEM of at least seven determinations from a representative experiment. *$P < 0.001$ versus untreated and jasplakinolide-treated cells. N.S., not significant compared to untreated control cells. C. Cell viability was determined using the trypan blue assay (Brogan *et al.*, 1994). Ltx-treated cells (■); ΔLtx-treated cells (□). Ltx-treated cells showed significantly greater cytotoxicity than its corresponding untreated control, while groups pretreated with either jasplakinolide or cD were not killed by Ltx. Values represent the mean ± SEM of three determinations from a representative experiment. *$P < 0.001$ versus cells receiving neither Ltx nor jasplakinolide or cD pretreatments.

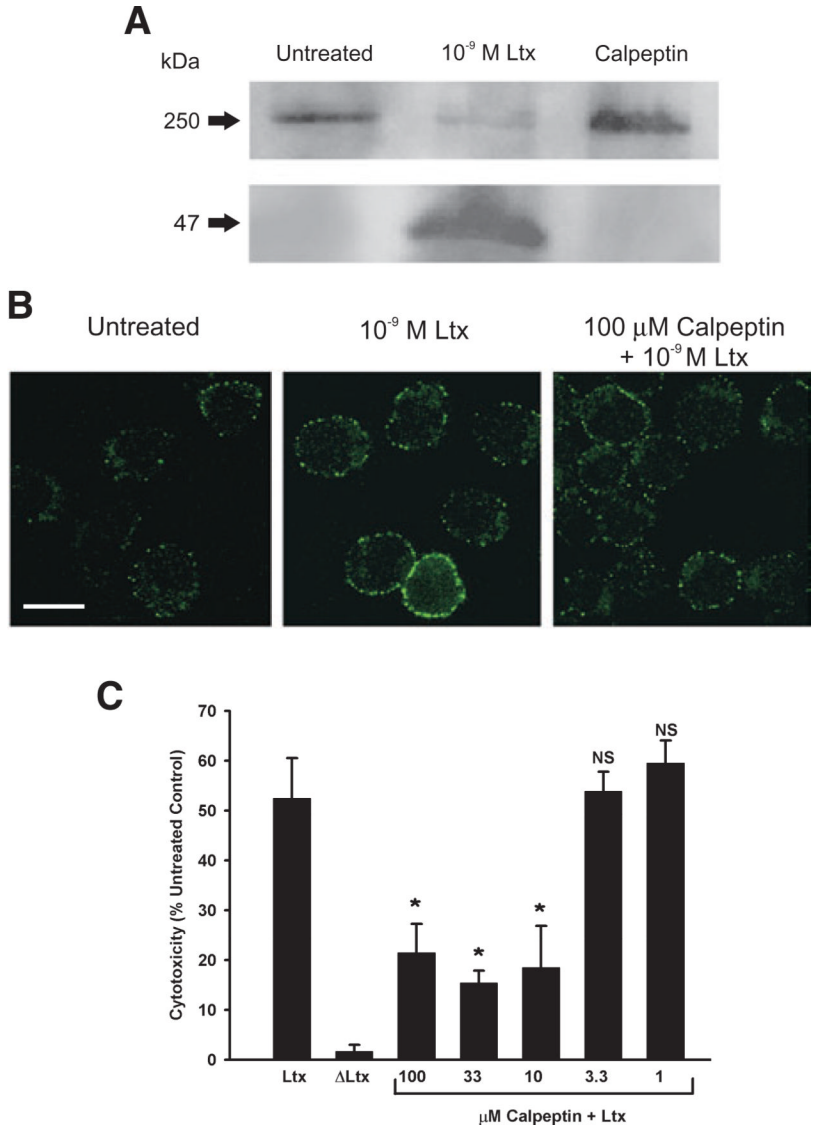

Fig. 5. Effect of calpain inhibition on Ltx-treated cells

A. The 47 kDa talin head proteolytic fragment resulting from cleavage of the 250 kDa intact talin protein was detected in a Western blot of the detergent-resistant membrane fraction of Ltx-treated cells with an antitalin monoclonal antibody (clone TA205). No talin cleavage was observed in untreated cells or Ltx-treated cells pretreated with calpeptin.

B. Cells were pretreated with 100 μM calpeptin (30 min, 37°C) before incubating with 10 μg ml^{-1} anti-CD11a and Ltx as in Fig. 1. In contrast to Ltx-stimulated cells, untreated cells and cells pretreated with calpeptin showed significantly lower levels of high intensity fluorescence (panel B and Table 2). Bar, 10 μm.

C. Cells were pretreated with 100, 33, 10, 3.3 or 1 μM calpeptin, before Ltx addition. Cells treated with Ltx and ΔLtx served as controls. Viability was determined using trypan blue exclusion assay and values represent the mean ± SEM of three determinations from a representative experiment. *$P < 0.001$ versus Ltx-treated cells; NS, not significant versus Ltx-treated cells.

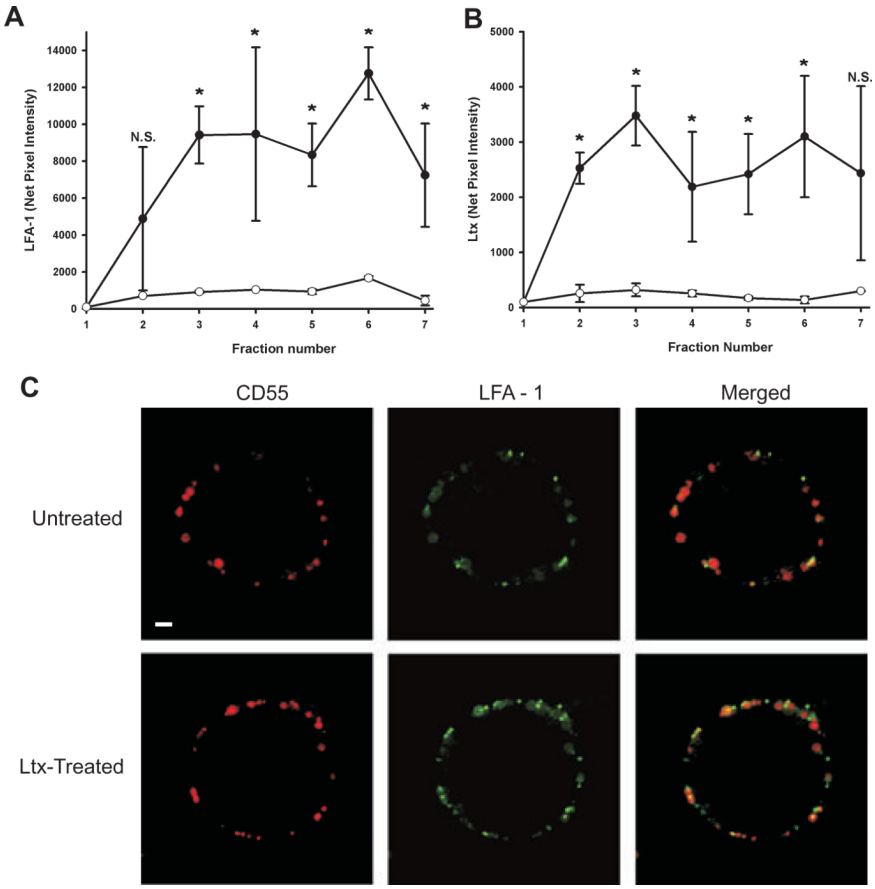

Fig. 6. Ltx and LFA-1 migrate to lipid rafts in Ltx-treated cells

A and B. Lipid raft fractions from sucrose density gradients were analysed using antibodies to LFA-1 (A) and Ltx (B). Western blots were scanned and the average pixel intensity was plotted against fraction number. Values represent mean ± SEM of three independent experiments. Significantly higher amounts of LFA-1 and Ltx were detected in raft fractions in Jn.9 cells exposed to 10^{-9} M Ltx (●) compared with untreated cells (○). *$P < 0.05$ and (N.S., not significant) versus untreated cells of each corresponding fraction.

C. Colocalization of LFA-1 (green) with the lipid raft marker CD55 (red) in Ltx-treated Jn.9 cells, in contrast to untreated cells. LFA-1 was detected as in Fig. 1. CD55 was detected using 20 μg ml^{-1} biotin labelled polyclonal goat anti-CD55 and Alexa Fluor®-647 conjugated streptavidin. Bar, 1 μm.

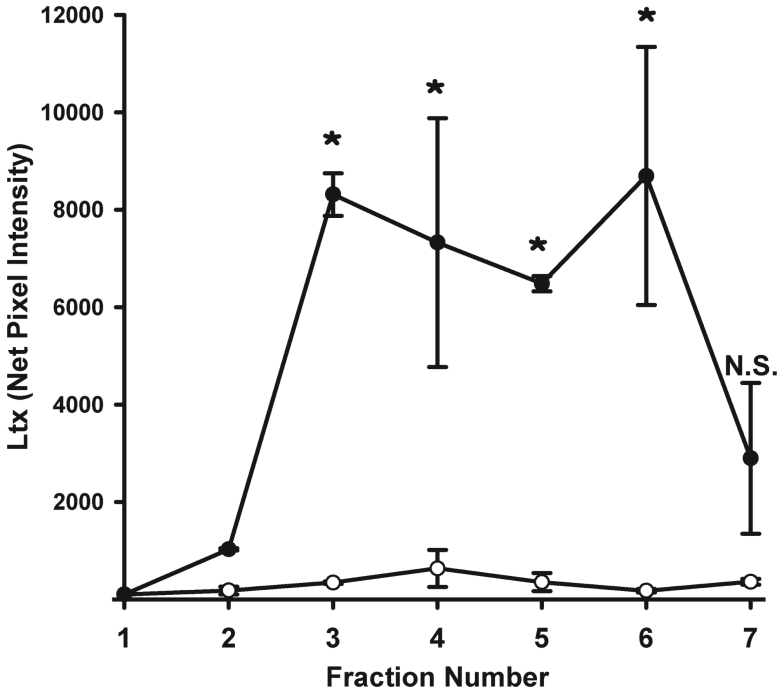

Fig. 7.

Cells expressing LFA-1 mobilize Ltx to lipid rafts. Ltx was detected in raft fractions of Jβ2.7/hCD11a (LFA-1 expressing) cells exposed to Ltx (●) but not in Ltx-treated mutant Jβ2.7 cells lacking LFA-1 (○). Ltx on the Western blots of lipid raft fractions were scanned as in Fig. 6. *$P < 0.05$ and (N.S., not significant) versus Ltx-treated Jβ2.7 cells of each corresponding fraction.

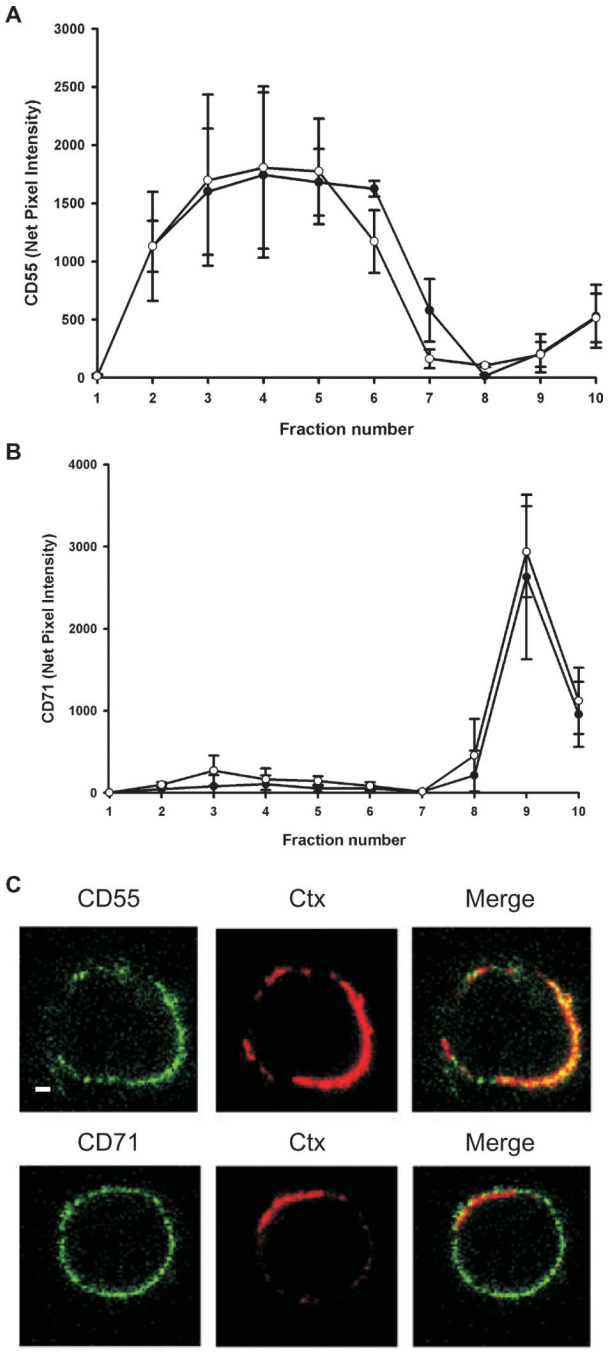

Fig. 8.

Analysis of lipid raft fractions. Fractions collected from the top of the gradient were run on SDS-PAGE and subjected to Western blot and probed with CD55 and CD71 antibodies. A and B. CD55 was detected in lipid raft fractions 2–7 (A), while CD71 was detected in non-raft fractions 8–10 (B), in the presence (●) or absence (○) of Ltx. The average pixel intensity of three independent experiments was obtained by scanning dot blots of lipid raft fractions with the Personal Densitometer SI using the Molecular Dynamics, version NT4, software. Error bars denote SEM ($P < 0.05$).

C. Confocal images of Jn.9 cells showing colocalization of cholera toxin (Ctx) with CD55 in lipid rafts and no colocalization with CD71. Bar, 1 μm.

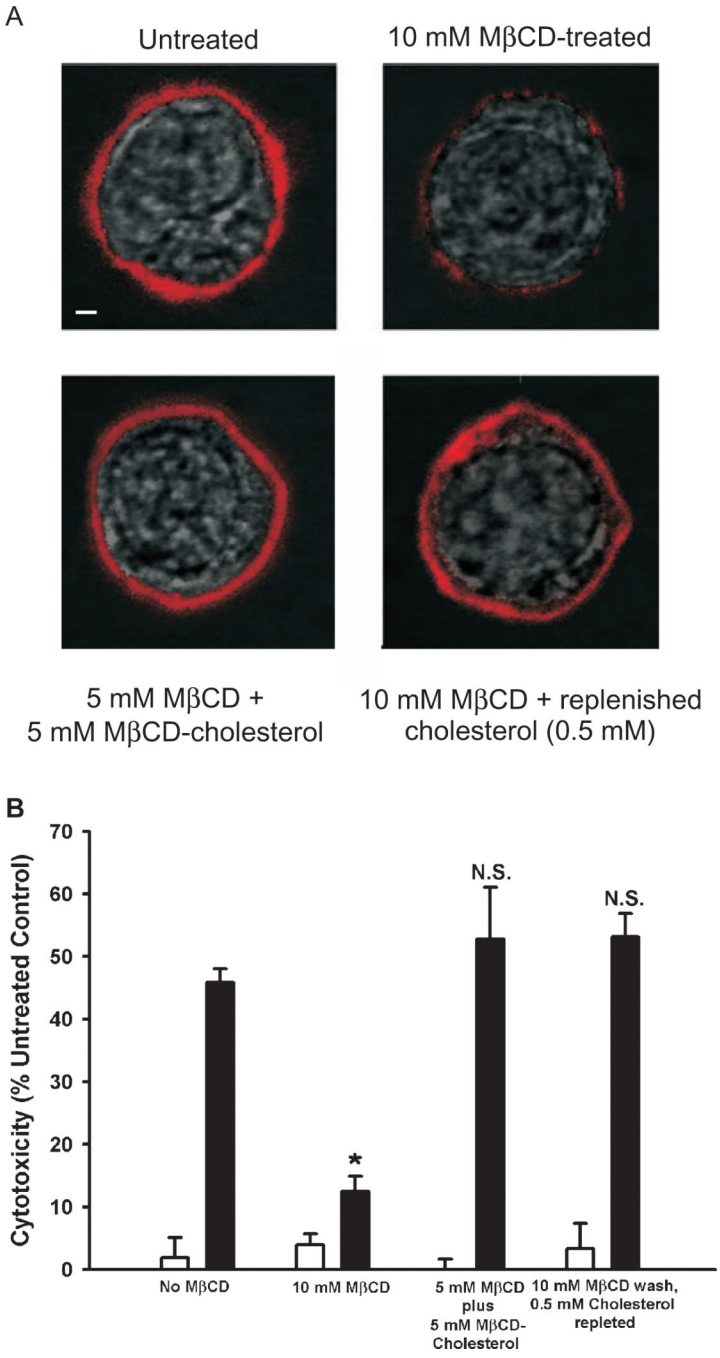

Fig. 9. MβCD treatment of Ltx-stimulated cells abolishes Ltx-mediated cytotoxicity

A. Jn.9 cells were subjected to various MβCD treatments before staining for lipid rafts as described in *Experimental procedures*. Bar, 1 μm.

B. Cells were subjected to the various MβCD treatments before incubating with 10^{-9} M Ltx (■) or ΔLtx (□). Surviving cells were counted and expressed as a percent of an untreated control. Values represent the mean ± SEM of three determinations from a representative experiment. $*P < 0.05$ versus cells treated only with Ltx; N.S., not significant versus cells treated only with Ltx.

Table 1

Net LFA-1 fluorescence intensity of Ltx-treated Jurkat cells.

Treatment	Average fluorescence intensity/cell
10^{-9} M Ltx	0.0145 ± 0.0028
Heat-inactivated 10^{-9} M Ltx	0.0044 ± 0.0004 *
Untreated	0.0057 ± 0.0009 *
Secondary antibody only	0.0002 ± 0.0001

Cells were incubated with anti-CD11a and 10^{-9} M Ltx at 37°C for 30 min, fixed and stained with Alexa Fluor®-488 conjugated secondary antibody. Fluorescence intensity for each sample was quantified using Metamorph® 6.0. Statistical analysis of these measurements is reported as mean ± SEM of 60 cells.

* $P < 0.05$ versus Ltx-treated cells.

Table 2

Calpeptin decreases Ltx induced LFA-1 clustering.

Treatment	Average fluorescence intensity/cell
10^{-9} M Ltx	0.0183 ± 0.0027
100 μM calpeptin + 10^{-9} M Ltx	0.00905 ± 0.0012 *
50 μM calpeptin + 10^{-9} M Ltx	0.0105 ± 0.0013 *
25 μM calpeptin + 10^{-9} M Ltx	0.0109 ± 0.0018 *
Untreated	0.00907 ± 0.0008 *
Secondary antibody only	0.0001 ± 0.00

Cells were pretreated with 100, 50 and 25 μM calpeptin for 30 min at 37°C. 10^{-9} M Ltx was added to cells and stained for LFA-1 as described in *Experimental procedures*. Fluorescence intensity for each sample was quantified using Metamorph® 6.0. Statistical analysis of these measurements is reported as mean ± SEM of 60 cells.

* $P < 0.001$ versus Ltx-treated positive control.

Table 3

Lipid raft cholesterol levels in normal and MβCD-treated Jn.9 cells.

Treatment	μM cholesterol/10^6 cells
None	1.86 ± 0.10
5 mM MβCD	1.23 ± 0.21 *
10 mM MβCD	0.95 ± 0.08 *
5 mM MβCD + 5 mM MβCD-cholesterol	5.17 ± 0.34
10 mM MβCD + 0.5 mM repleted cholesterol	6.82 ± 0.20

Jn.9 cells were subjected to one of four MβCD treatments at 37°C for 30 min. Untreated cells served as a control. The cholesterol content of lipid rafts from MβCD-treated and untreated cells was determined using a Amplex Red Cholesterol Assay Kit (Molecular Probes, Invitrogen). Values represent mean ± SEM of three separate experiments.

* $P < 0.01$ versus untreated Jn.9 cells.